gases

MDPI

Article

Towards the Isothermal Gas Compression—A Novel Finned Piston-Cylinder with Increased Efficiency

Alfred Rufer

EPFL Swiss Federal Institute of Technology in Lausanne, 1015 Lausanne, Switzerland; alfred.rufer@epfl.ch

Abstract: In this paper, a novel concept of a finned piston system is presented and analyzed in which the compression heat is continuously extracted from the compression chamber. The resulting compression characteristic moves in the direction of an isothermal process, reducing the temperature of the compressed fluid in the compression chamber and reducing the necessary mechanical work required to carry out the process. The finned piston concept consists in an integrated heat exchanger inside of the chamber that is constituted of imbricated flat fins placed on the stator part and on the mobile piston. The internal heat exchange on the surface is strongly increased in comparison with a classical piston/cylinder. The energetic performance of the new system is evaluated with the help of simulation. The pressures, forces, and temperature of the compressed gas are simulated as well as the mechanical work needed. The different curves are compared with the system's adiabatic and isothermal characteristics.

Keywords: gas compression; isothermal; energy efficiency; heat exchange; finned piston

1. Introduction

In the context of climate change and reducing green gas emissions, many efforts are being made to establish new alternative sources. From photovoltaic plants to wind energy farms, high investments are being made towards replacing fossil-based solutions. As a possibility to bridge or compensate for weather or seasonal fluctuations, long-term storage technologies will be based on energy conversion into chemical carriers as such as hydrogen, synthetic gases, or fuels. In such energy chains, gas compression stages will be used intensively and will have to be further developed to show higher energy efficiencies than the industrial solutions known today.

Not only for new energy applications but also in many other industrial processes, compression machines are used today as objects where energy efficiency issues have not been at the forefront of their technical developments. In a more general context, improvements in the energetic performance of compression machines and other machines or processes will be part of the solutions of the energy transition. [1–3].

In this paper, an original solution for the realization of compression stages is presented and analyzed. The new concept, called the finned piston, is based on the principle of continuously exporting the heat produced by the compression mechanism itself in order to reduce the amount of mechanical work needed for the elevation of the pressure following the reduction in the volume in the compression chamber. The concept of the finned piston has a heat exchanger integrated in the compression chamber. The new geometry proposed in this paper is following a previous study proposed by Mahbod Heidary in his PhD thesis [4–6]. The use of imbricated cylindric fins in the stator part of the cylinder as well as on the sliding piston significantly increases the convective heat exchange on the surface in comparison to a classic piston/cylinder assembly and allows a compression process with a reduced elevation of the temperature inside the compression chamber [7–10].

The principle of the finned piston is applied on a so-called gas booster, used in many applications, with low power and high pressure. Whereas the original gas boosters

check for updates

Citation: Rufer, A. Towards the Isothermal Gas Compression—A Novel Finned Piston-Cylinder with Increased Efficiency. *Gases* **2024**, *4*, 59–73. https://doi.org/10.3390/gases4020004

Academic Editor: Ben J. Anthony

Received: 13 February 2024
Revised: 14 March 2024
Accepted: 4 April 2024
Published: 8 April 2024

use pneumatic actuators, well-known for their very low efficiency, a first important step has been achieved by replacing these with a variable-speed electric motor completed by an active compensator for the low-frequency power fluctuations. Figure 1 shows the evolution of the gas booster from its original version with a pneumatic motor (a) to the electromechanically moved versions. Two solutions are proposed, the first using a conventional crankshaft and piston rod (b), and the second using a so-called Scotch Yoke mechanism (c) [11,12]. The next step for an increased efficiency is an improvement in the thermodynamic mechanism of the compression itself, which attempts to reach a characteristic of isothermal compression.

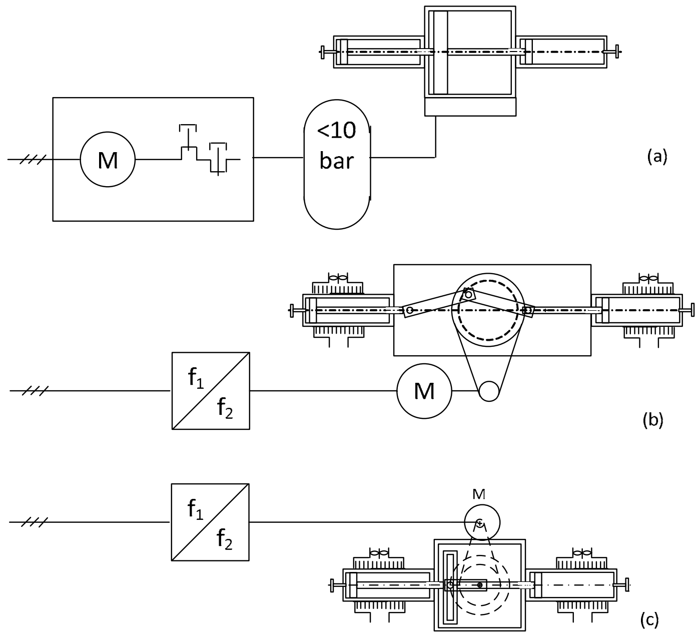

Figure 1. Gas boosters driven by pneumatic motor (**a**), and by electric motor (**b**,**c**).

2. The Compression Cylinder Based on a Finned Piston

In comparison with a classical cylinder/piston assembly, a so-called finned piston concept is built of imbricated metallic fins, with a first part at the stator side and a second one on the side of the sliding piston. The original system analyzed in [4–6] used imbricated cylindric fins as represented at the bottom of Figure 2. One can see that such an architecture uses nearly double the space of a classical cylinder/piston system (top of Figure 2) when the volume occupied by the cooling fins is identical to the volume of the compression chamber. The gas is compressed in the spaces between the stator fins, where the fins of the mobile part play the role of small pistons. The intake and exhaust path is given through the radial perforations from fin to fin, and via the outlet (O1 in Figure 2). On the other side (piston side), the gas is compressed in the spaces between the fins of the mobile part where the stator fins play the role of pistons. The intake and exhaust path is given on that side by radial perforations from fin to fin at the rear side of the piston fins and through a second outlet perforation placed at the top end (right side) of the stator fins (O2 in Figure 2). Anti-return valves in the intake and exhaust paths should be placed just after the orifices O1 and O2 in order to avoid excessive dead volumes. The gases of the two sides can then be mixed by a dedicated collector.

The system analyzed in this paper is built of imbricated flat fins, as represented in the middle of the figure. The advantage of using flat fins instead of cylindric ones will be explained in the next section.

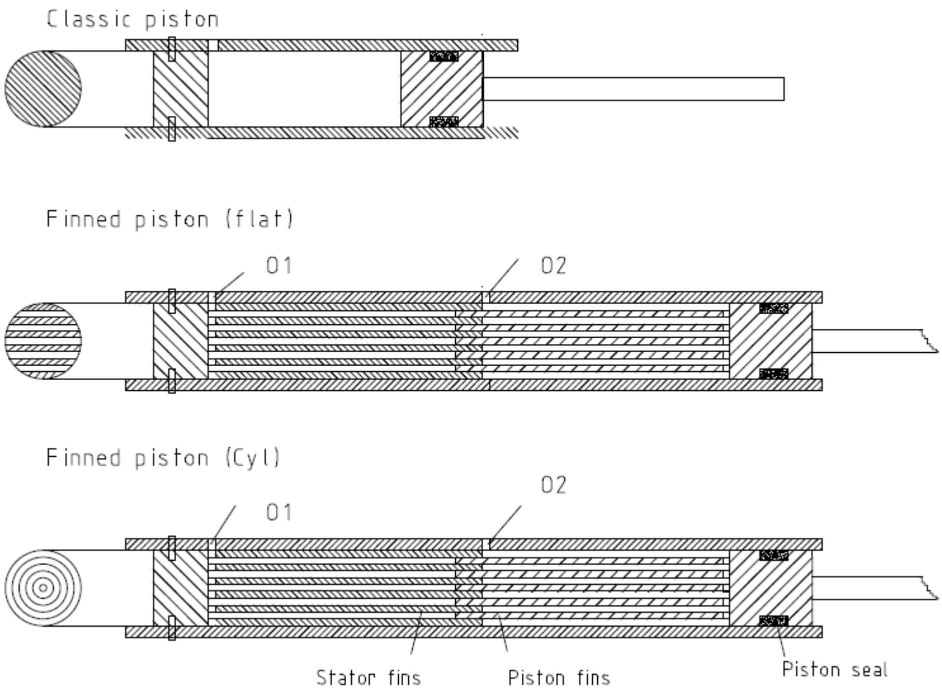

Figure 2. Classic piston and finned pistons with flat and cylindric fins.

2.1. The Heat Exchange Surface of the Classic, Flat and Cylindric Fin Systems

The heat exchange surface of the different systems comprises the external surface of the global compression cylinder, the end and front surfaces of the stator and piston, and also the effective side surface of each fin. A comparison of the three systems is given on the basis of a specific system, with the parameters given in Table 1.

Table 1. Dimensions of the system.

Cyl Internal Diameter	Fin Thickness	Active Length of the Cylinder	Stroke
D = 27.5 mm	h = 2.5 mm	L = 100 mm	90 mm

2.1.1. Heat Exchange Surface of the Classical Cylinder

The convection surface of the classical cylinder–piston assembly is equal to the sum of the extreme surfaces and the external cylinder surface, with

$$S_{extreme} = 2 \cdot \pi \cdot r^2 = 2 \cdot \pi \cdot (27.5/2)^2 = 1187 \text{ mm}^2 \quad (1)$$

and

$$S_{ext\_cyl} = 2 \cdot \pi \cdot r \cdot l = 2 \cdot \pi \cdot (27.5/2) \cdot 100 = 8639 \text{ mm}^2 \quad (2)$$

$$S_{tot\_classic\_cylinder\_without\_fins} = 1187 + 8639 = 9826 \text{ mm}^2 \quad (3)$$

This surface varies depending on the piston's position between 9826 mm^2 and 1187 mm^2.

2.1.2. Heat Exchange Surface of the Flat Fin Cylinder

This surface is calculated according to the representation in Figure 3.

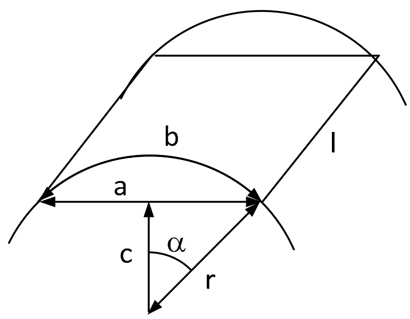

Figure 3. Parameters of the flat fin cylinder.

The surface of a fin side is given by

$$S = a \times l \tag{4}$$

where a is the fin's width and l is the stroke of the piston in the cylinder:

$$a = 2 \times r \sin(\alpha) \tag{5}$$

the angle α is

$$\alpha = arc \cos\left(\frac{c}{r}\right) \tag{6}$$

and the fin's width can be calculated as

$$a = 2 \times r \times \sin\left(arc \cos\left(\frac{c}{r}\right)\right) \tag{7}$$

The 11 fins totalize a surface of 46,145 mm^2.

To this surface, the front and rear surface must be added, namely $S_{extrem} = 1187$ mm^2 given by (1), as well as the surface of the external cylinder $S_{ext\_cyl} = 8639$ mm^2 from (2)

Finally, the total convection surface of the flat fin piston–cylinder assembly is

$$S_{tot\_flat\_fins} = 46,145 + 1187 + 8639 = 55,971 \text{ mm}^2 \tag{8}$$

The details of the calculation are given in Appendix A.

2.1.3. Heat Exchange Surface of the Cylindric Fin Cylinder

The convection surface of the cylindric fins system is calculated in Appendix B.

The external surface is equal to

$$S_{tot\_\text{cylindric}\_fins} = 39,250 + 1187 + 8639 = 49,076 \text{ mm}^2 \tag{9}$$

2.1.4. Comparison of the Different Heat Exchange Surfaces

The heat exchange surfaces of the three solutions (classical, flat fins, and cylindric fins) are represented in Figure 4, and are dependant on the position of the piston.

Figure 4 shows an important property of the classical cylinder–piston system, where the heat exchange surface reaches its maximum value at the BDC (bottom dead centre) position (corresponding to the 0 and 1 value of the dimensionless piston travel time of the cycle represented in the figure). The minimum value of the surface is given at the TDC (top dead centre) position (corresponding to the 0.5 value of the dimensionless piston travel time in the figure).

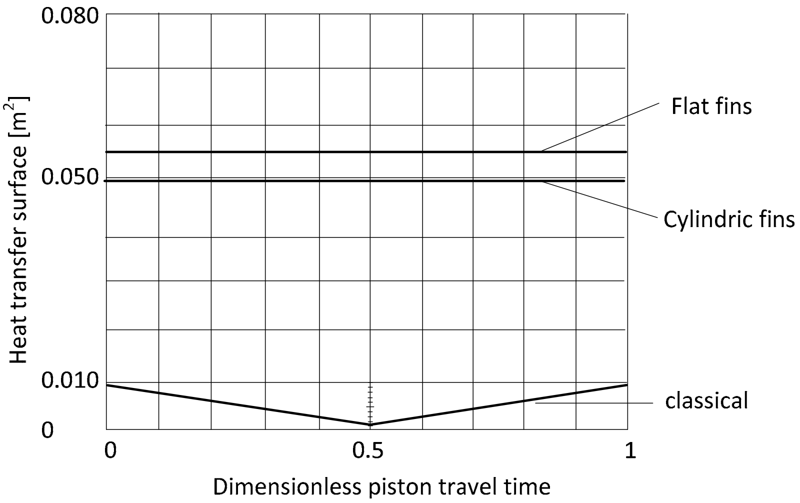

Figure 4. Heat transfer areas of the different cylinders.

For the finned pistons (flat fins and cylindric fins), the heat transfer surface remains constant and independent of the position of the piston since there is a gap between the fins, and this allows the heat transfer to occur on the entire fin surface (Figure 4). However, the effective thermal resistance for the heat transfer from the compressed gas to the surrounding area will be calculated in Section 3.1.2 and is dependant on the piston's position.

3. Two Models for the Simulation of the Finned Piston

Two different methods can be applied for the evaluation of the performance of the compression cylinder. The first method is based on a common expression of the variation in the pressure resulting from the variation in the volume of the chamber:

$$P_{gas} = P_{in\_gas}\left(\frac{V_{comp\_\max}}{V_{compr\_\mathrm{var}}}\right)^{\gamma} \tag{10}$$

with γ = 1.4 in the adiabatic mode and γ = 1 in the isothermal.

For an implementation of this expression, the volumetric ratio must be known, and it is relatively easy to define as a time function for representing the time variation in the pressure. The polytropic factor γ indirectly represents the quality of the thermal flow from the compressed gas to the surrounding area but does not allow us to make a relation to the thermal model based on classic parameters like the thermal capacity of the compressed gas, nor the thermal resistance (which is easy to calculate on the basis of the known parameters of the geometry of the finned system). For the evaluation of the temperature of the gas, another expression can be used:

$$T_{gas} = \frac{T_{in}}{\left(\frac{V_{compr\_\mathrm{var}}}{V_{comp\_\max}}\right)^{\gamma-1}} \tag{11}$$

Again, in this case, the polytropic factor must be known, and it cannot be calculated from the parameters of a thermal model. With these formulas, the evolution of the pressure and of the temperature can be drawn, depending on the variation in the volume for the simple cases of adiabatic or isothermal compressions.

A second method which is based on the general expression $P \cdot V = m \cdot R \cdot T$ can be used and can be implemented in the form of the structural diagram of Figure 5.

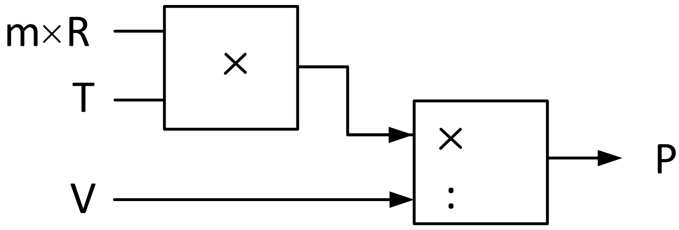

Figure 5. Thermal model for the pressure.

For this model, the temperature of the gas can be introduced as an output variable of a thermal model. Such a model is simply established on the basis of two known parameters, namely the thermal capacity of the gas and a thermal resistance which defines the thermal flow to the external world. The input variable of the thermal model corresponds to the thermal power transmitted to the gas and is calculated from the piston's velocity and the piston's force. The mechanical power Pow exerted by the piston on the gas is supposed to be identical (friction is neglected) to the transmitted thermal power P_{th}, as long as the exhaust valve of the cylinder is closed and no fluid in transferred out of the cylinder. The complete system model is represented in Figure 6, where the equivalent scheme for the thermal model with capacitor C_{th} and resistance R_{th} is transformed in a structural diagram with the integration block (1/s). The output variable of the thermal model corresponds to the temperature of the gas and, in the equivalent scheme, corresponds to the voltage across the thermal capacitor C_{th}. The auxiliary (binary) variable X represents the opening/closing of the exhaust valve.

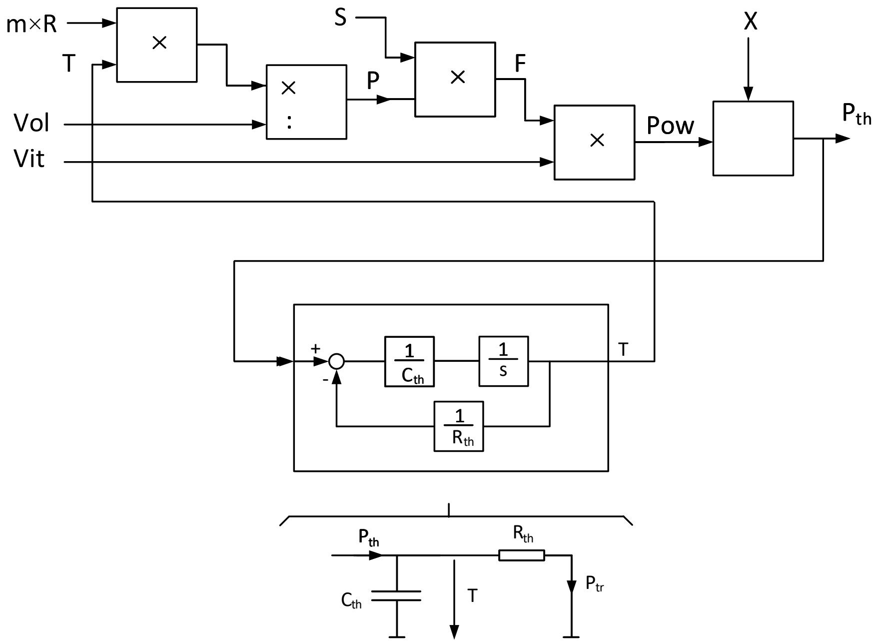

Figure 6. The complete model for the compression cylinder with the thermal part.

3.1. Parameters of the Thermal Model of the Finned Piston System

The energetic performance of the finned piston system will be evaluated with the help of a simulation of one compression stroke. First, the evolution of the temperature of the gas will be simulated and, second, the necessary mechanical work needed for the compression will be calculated. These results will be obtained from the system model represented in Figure 6, where the parameters of the thermal model will play a significant role. The two parameters C_{th} and R_{th} will be calculated for the example that is defined in Table 1. They are based on the mass of the gas that is compressed and on the variable thermal resistance of the exchange between the fins and within the interspace between fins, as well as being dependent on the piston's position.

3.1.1. Thermal Capacitance

The thermal capacitance C_{th} is expressed as J/K and is calculated through Equation (12)

$$C_{th} = m \cdot c_v \tag{12}$$

with the value of the mass of the gas m which is calculated from the filling conditions of the cylinder at a pressure of 15 bar and at ambient temperature

$$m = \frac{p \cdot V}{R \cdot T} = \frac{15 \cdot 10^5\ \mathrm{N/m^2} \cdot 53.5 \cdot 10^{-6}\ \mathrm{m^3}}{0.287\ \mathrm{kJ/(kg \cdot K)} \cdot 293\ \mathrm{K}} = 9.54 \cdot 10^{-4}\ \mathrm{kg} \tag{13}$$

This results in:

$$C_{th} = m \cdot c_v = 9.54 \cdot 10^{-4}\ \mathrm{kg} \cdot 0.718\ \mathrm{kJ/(kg \cdot K)} = 0.682\ \mathrm{J/K} \tag{14}$$

3.1.2. Thermal Resistance

The thermal resistance which defines the heat transfer from the heated gas to the surrounding area results from the parallel connection of two resistances, R_{th1} and R_{th2}. R_{th1} corresponds to the transfer in the space between fins (dominant when piston is deployed, BDC). R_{th2} corresponds to the gaps between the fins (dominant when the piston is retracted, TDC). The two resistances are represented in Figure 7.

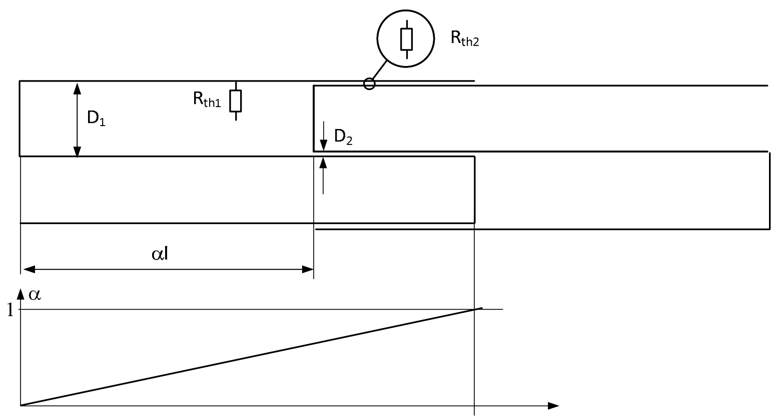

Figure 7. Definition of the thermal resistances R_{th1} and R_{th2}.

The two resistances vary based on the function of the position and are calculated as:

$$R_{th1} = \frac{1}{H_1 \cdot \alpha A} \tag{15}$$

$$R_{th2} = \frac{1}{H_2 \cdot (1-\alpha)A} \tag{16}$$

A represents the value of the total heat exchange surface, namely the sum of the surface of the fins, added to the surface of the piston's front and back, and also the surface of the outer wall. The factor α changes from zero to one depending on whether the piston is deployed or retracted.

H_1 and H_2 are the thermal transfer coefficients expressed in $\mathrm{W/(m^2 \cdot K)}$

$$H_1 = \frac{k_a}{D_1/2} \tag{17}$$

$$H_2 = \frac{k_a}{D_2/2} \tag{18}$$

where k_a is the thermal conduction coefficient of the gas (air in the simulated case) expressed in W/(m·K). D_1 and D_2 are the distances between the fin walls, as represented in Figure 7.

Finally, the value of the global R_{th} is obtained by the calculation of the parallel connection of R_{th1} and R_{th2}, according to

$$R_{th} = \frac{R_{th1} \cdot R_{th2}}{R_{th1} + R_{th2}} \tag{19}$$

R_{th} is represented in Figure 8 as a function of the displacement of the piston in the cylinder.

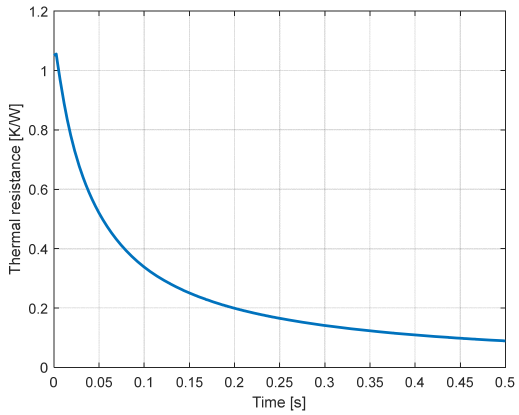

Figure 8. Thermal resistance as a function of the piston's displacement.

4. Simulation Results

4.1. Simulation Conditions

A finned piston–cylinder with flat fins as represented in the middle of Figure 2 is simulated in the time domain with the parameters given in Table 1. The simulation covers one half-period of the cycle and corresponds to the compression stroke with a constant velocity of the piston. The simulation time is 0.5 s. The corresponding variation in the volume is represented in Figure 9.

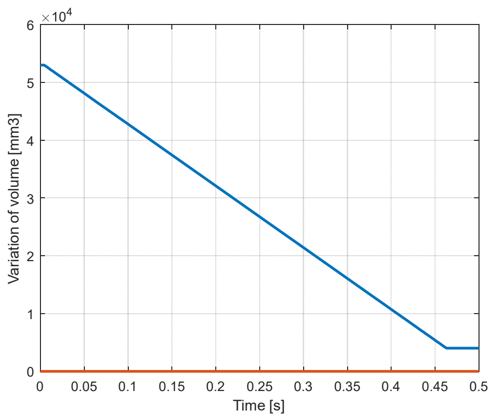

Figure 9. Variation in the volume of the compession chamber.

The limitation of the volume at the TDC (top dead centre) is imposed intentionally to avoid the infinite value of the ratio $V_{comp\_\max}/V_{compr\_\mathrm{var}}$ in the simulation.

Figure 10 gives, first, a comparison of the two models used for the calculation of the pressure (Equation (9) and Figure 5). The comparison is made for an isothermal compression. In this comparison, the elevation of the pressure goes up to the limit imposed by the volume reduction limit. For the following simulations, the pressure is limited to a value of 160 bar, which corresponds to the opening of the exhaust valve when the pressure of the gas in the cylinder equals the pressure in the receiving reservoir. The initial value of the pressure (intake) is 15 bar. The curves of the two models are completely superimposed.

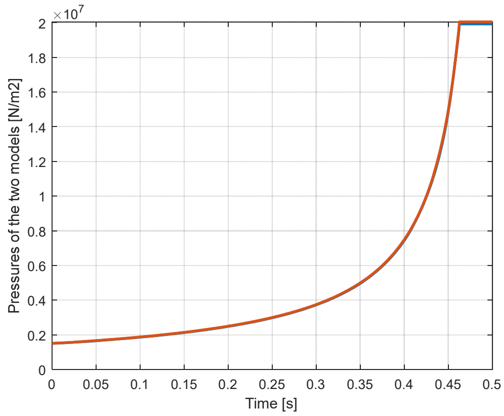

Figure 10. Comparison of the models.

4.2. Pressures, Forces and Temperatures

In Figure 11, three curves for the elevation of the pressure are given. First, the pressure elevation in the adiabatic mode is shown, where the whole compression heat is maintained inside of the cylinder (blue curve). The initial condition is a value of 15 bar (15×10^5 N/m^2). When the pressure reaches the value of the external reservoir (160 bar), an anti-return valve opens automatically and the remaining portion of the stroke occurs under this pressure value when the compressed gas is transferred. The second curve (yellow curve) corresponds to a model of the compression according to the diagram of Figure 6. The temperature of the gas is calculated with the help of a thermal model using the parameters of the thermal capacity of the gas and the variable value of the thermal resistance, which were calculated in Section 3.1.2. The curve shows a typically slower rise of the pressure due to the continuous evacuation of a part of the produced heat. The third curve (red curve) corresponds to an isothermal compression.

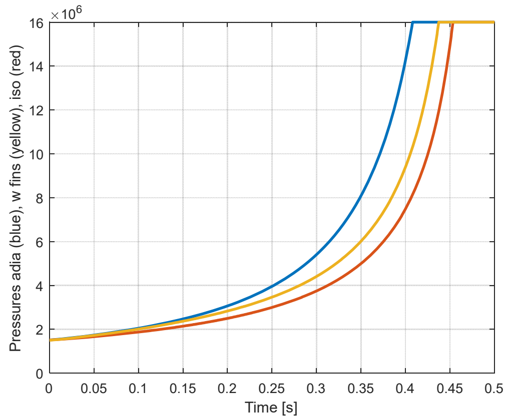

Figure 11. Pressure during compression: adiabatic, finned, and isothermal.

Figure 12 shows the variation of the force exerted by the piston on the gas. Again, the three conditions are represented, adiabatic (blue), finned piston (yellow) and isothermal (red).

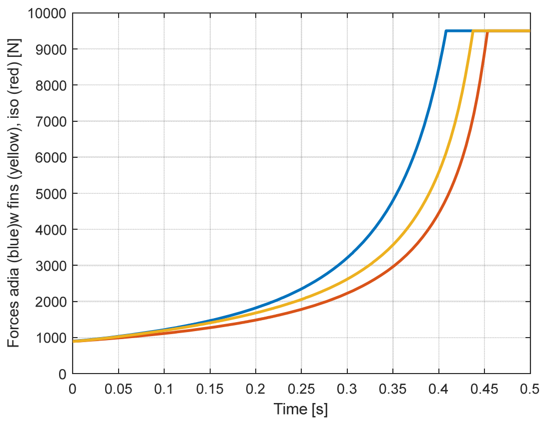

Figure 12. Forces during compression.

In the simulation diagram of Figure 6, the mechanical power (Pow) and the power transmitted to the gas (P_{th}) are simulated. The evolution of these two variables is represented in Figures 13 and 14. The mechanical powers are calculated from the mechanical force and the velocity of the piston. After the opening of the exhaust valve, the power exerted by the piston serves to exhaust the gas and no more energy is transmitted to the gas in the cylinder. The opening of the valve is activated in the simulation diagram by the binary variable X.

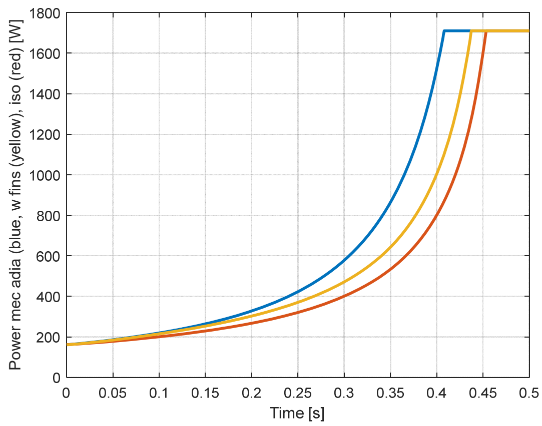

Figure 13. Mechanical power needed by the piston.

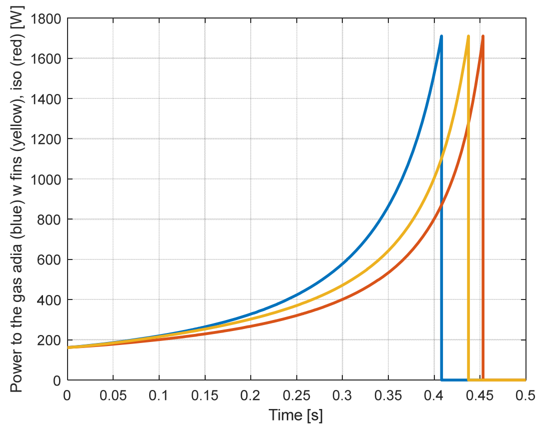

Figure 14. Power transmitted to the gas.

Figure 15 represents the principal result of this study, namely the curves of the elevation of the temperature in the compression cylinder. The yellow curve shows the performance of the proposed system using the finned piston technology. The blue and the red curves represent the temperatures of the gas in the conditions of adiabatic and isothermal compression, respectively. The performance of the integrated heat exchanger (the finned system) is particularly visible through the strong reduction in the elevation of the temperature (around 100 K instead of nearly 250 K in adiabatic conditions).

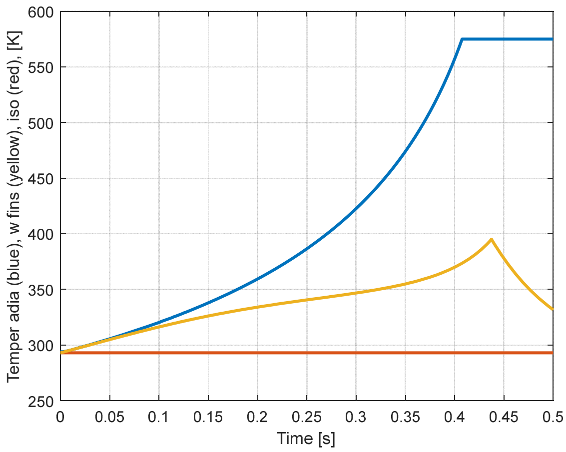

Figure 15. Temperatures of the gas during compression.

Effect of a Reduced Speed

Reducing the speed of the piston has the effect that the evacuation of the compression heat is more performant due to the fact the thermal time-constants in the thermal model (C_{th} and R_{th}) are not changed. The result of this is that the rise in the temperature in the cylinder is reduced. Figure 16 shows, again, the evolution of the temperature when the speed of the piston is reduced from 0.18 m/s to 0.09 m/s (Figure 16a) and 0.045 m/s, respectively (Figure 16b). This means that the 90 mm stroke is covered in 1 and 2 s (instead of 0.5 s). The value of the temperature in adiabatic conditions is unchanged as well in isothermal conditions. For the finned piston system (yellow curve), the elevation of the temperature is one half of the elevation with the original speed (0.18 m/s). With a speed of 0.045 m/s, the elevation is reduced by another 50%.

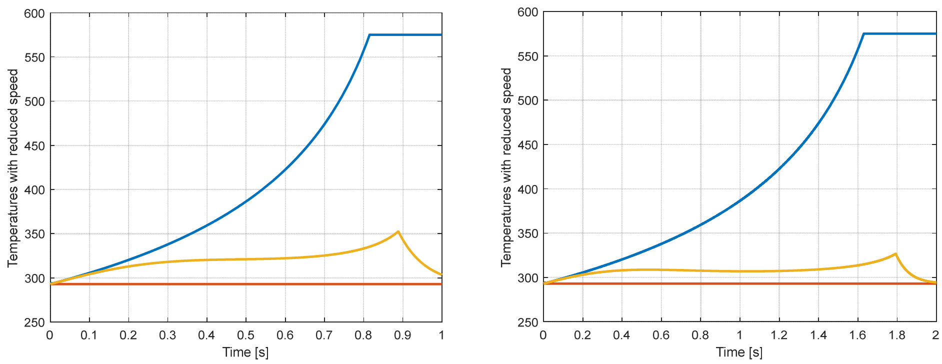

(**a**) (**b**)

Figure 16. Temperatures with reduced speed: (**a**) 0.09 m/s, (**b**) 0.045 m/s. Adiabatic (blue), finned (yellow), and isothermal (red).

4.3. Energetic Considerations

Figure 17 shows the performance of the finned piston system in terms of energy. The three curves correspond to the integration of the mechanical power needed to move the piston. It is effectively the energy consumed by the different compression tasks (adiabatic in blue, finned in yellow, and isothermal in red). The reduction in the needed energy from 350 to 300 joules corresponds to a saving of 14%.

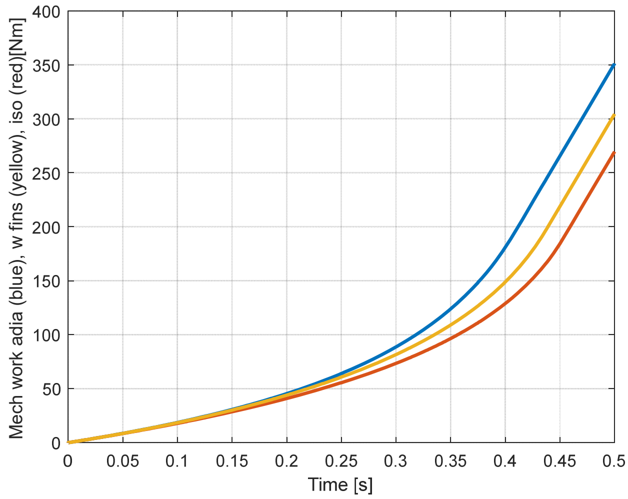

Figure 17. Mechanical work for the compression.

In Figure 18, the energy transferred from the piston to the gas is represented. This energy comprises two parts, namely the energy transferred to the gas itself (gas internal energy) and a part which is evacuated by the fins.

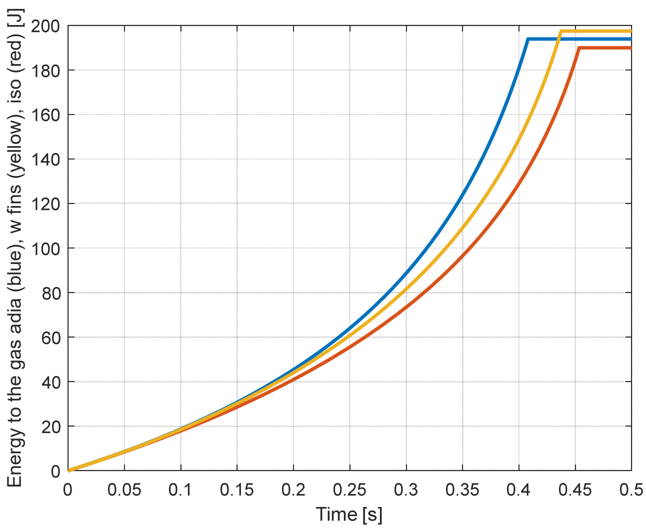

Figure 18. Energy transferred from the piston to the gas in the cylinder.

Effect of a Reduced Speed

The mechanical work needed for the compression up to 160 bar is also reduced when the compression speed is reduced. Figure 19 shows the same variables as in Figure 17 but for when the speed is reduced to 0.09 m/s (Figure 19a) and 0.045 m/s (Figure 19b), respectively. The final value of the work of the finned piston at t = 1 s is 289 J for a piston speed of 0.09 m/s. The reduction from 350 J to 289 J represents a reduction of 17.4%. For a speed of 0.045 m/s (Figure 19b), the curve of the work of the finned solution is even closer to the curve of the isothermal compression (final value: 279 J).

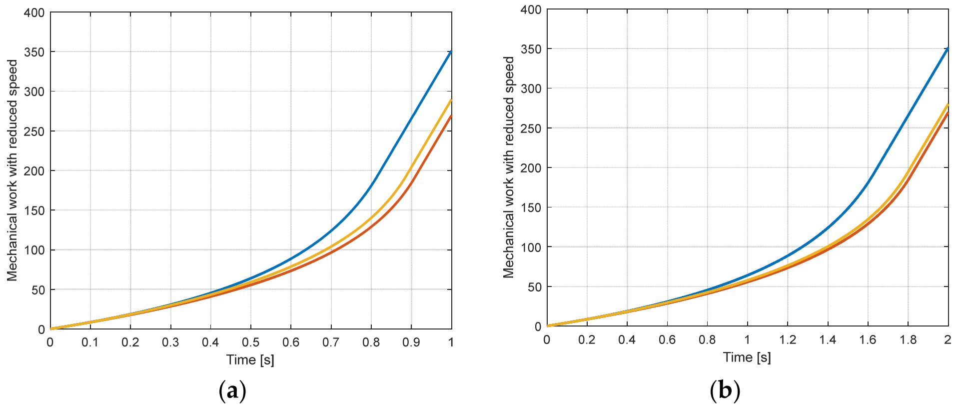

Figure 19. Mechanical work with reduced speed: (**a**) 0.09 m/s, (**b**) 0.045 m/s. Adiabatic (blue), finned (yellow), and isothermal (red).

5. Discussion and Future Development

5.1. The Limit of the Model of the Finned Piston Systems

The energetic performance of the finned piston concept has been evaluated by simulation on the basis of a dedicated model which includes a thermal model for the cooling effect of the finned system. The gain in the necessary mechanical work for the compression has been evaluated in this first study. Additionally, the elevation of the temperature and the mechanical work for compression has been simulated for a reduced speed of the piston. The verified performance of the proposed system with the simple model used in this study shows good potential for the performance increase of a real system. However, the performance should be calculated more accurately, including, for instance, the friction of the mechanical parts, especially of the sealing elements. Particularly for high pressures, the influence of the seals can be of importance.

All the simulated phenomena and, in the foreground, the elevation of the temperature are based on the assumption that the temperature of the fins and of the whole cylinder body is constant and identical to the ambient temperature. In reality, the temperature of the fins will be dependent on the quality of their own cooling. In consequence, the model should be completed by a part dedicated to the cooling of the stator fins and of the mobile fins. Such a model should include the resistance of the thermal conduction of the element between the compression fins and the fins of the stator and mobile cooling system. Also, the thermal capacitance of the additional elements should be included.

5.2. A Finned Compressor with Cooling of the Stator and of the Mobile Finned Piston

In Figure 20, a complete compressor with the finned technology is represented. The compressor consists of two cylinders using the finned technology. The two pistons are connected to a common crankshaft via two connecting rods, and they work with a 180° phase-shift. This phase-shift allows us to get the same compression sequence of the two lateral cylinders of a classical gas booster, shown in Figure 1.

The cooling of the stator part does not represent a big challenge due to its non-moving character. However, concerning the sliding finned pistons, the transfer of the heat is of a different difficulty. The heat transfer functional elements are given by a couple of sliding horizontal fins, moving inside a cylinder-prolongation section, and are cooled by a transverse air flow. The air flow is produced by a dedicated fan.

The sliding fins play two different roles, the first being to cool the piston at its rear side, and the second being to transmit the compression force from the crankshaft to the mobile piston.

The proposed system in Figure 19 should be modelled accurately for an evaluation of its performance. A finite element representation of the thermodynamic phenomena will certainly produce the best results.

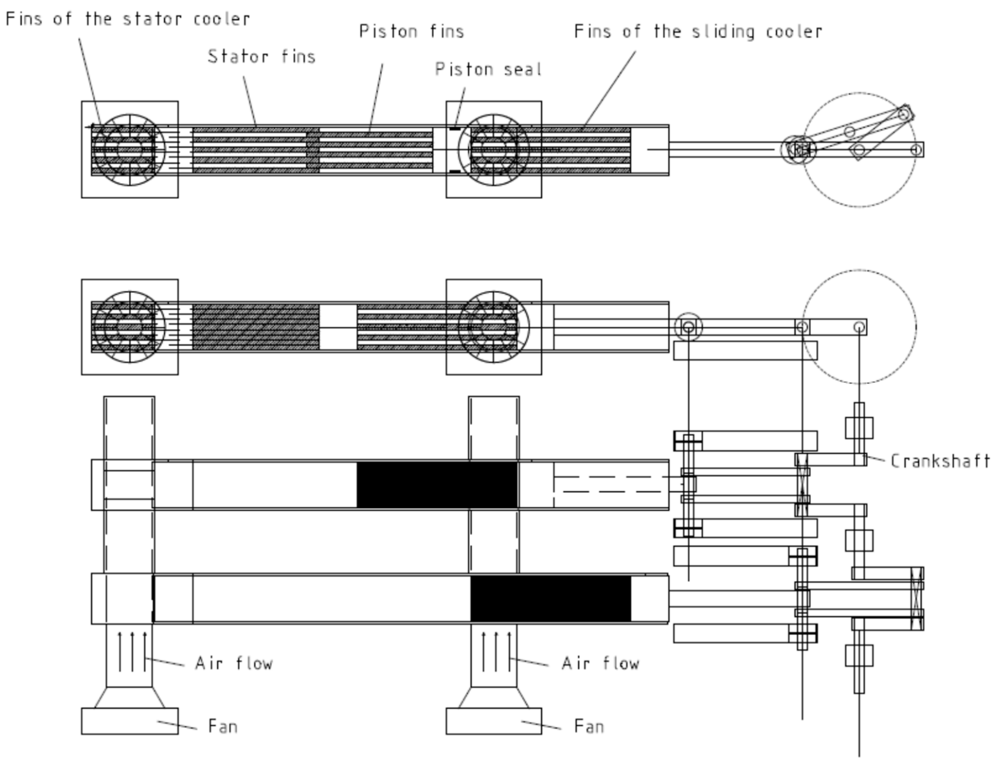

Figure 20. Compressor with two cylinders (180° phase-shift) and cooling of the fins.

6. Conclusions

A new finned piston system has been analyzed for its energetic performance and for its reduction in the elevation of the temperature. The aim of this study is to develop a cylinder/piston system for which the compression characteristic tends to move in the direction of an isothermal compression. The technique used is to integrate a heat exchange device inside of the compression volume, allowing a permanent evacuation of the produced heat during the compression process. The heat exchange device consists of imbricated fins sliding with the piston movement against the fins of the stator part. The heat transfer area of a system with flat fins is compared to a system with cylindric fins, showing a superior performance of the former system. This study illustrates a simplified system with a linear movement of the piston. The thermodynamic phenomena are represented with simple thermodynamic relations, where ideal adiabatic conditions are simulated as well as ideal isothermal phenomena. The new proposed system with fins is evaluated using an integrated thermal model of the heat exchange and shows a good performance and significant reduction in the temperature in the compression cylinder. The simulations are made for different values of the compression speed. The reduction in the compression speed shows a clear tendency of performance increase, namely reduction in the needed mechanical effort together with a reduction in the temperature of the compressed gas.

Funding: This research received no external funding.

Data Availability Statement: Data available on request.

Conflicts of Interest: The authors declare no conflict of interest.

Appendix A

The convection surface of a 27.5 mm cylinder with 2.5 mm flat fins is calculated.

Flat Horizontal fins D=27.5, Fin_th=2.5 (11 fins)

D	2xC	α [rad]	α [deg]	sin(α)	a	S	S_horiz_tot	S_ext_arc	S_ext_lat	2xS_ext_lat
								0		
27.5	22.5	0.6125547	35.114603	0.5749596	15.811388	1581.13883		1684.52553	1684.5255	3369.0511
27.5	17.5	0.8810213	50.504407	0.7713892	21.213203	2121.320344		2422.808647	738.28312	1476.5662
27.5	12.5	1.0989345	62.996245	0.8907235	24.494897	2449.489743		3022.069846	599.2612	1198.5224
27.5	7.5	1.2945697	74.211002	0.9620914	26.457513	2645.751311		3560.066664	537.99682	1075.9936
27.5	2.5	1.4797615	84.827095	0.9958592	27.386128	2738.612788		4069.344259	509.27759	1018.5552
						11536.31302	46145.252	0	4069.3443	8138.6885
								0		
27.5	-2.5	1.6618311	95.264203	0.9958592	27.386128	2738.612788		4570.035538	500.69128	500.69128
							Lateral surface (S_ext_lat_tot			8639.3798
							Surface_of-the_extremities			1187.3125
							Total_conv_surface			55971.944

Figure A1. Details of th calculation of surfaces of the flat finned piston.

Appendix B

Calculation of the convection surface of the cylindric fins.

Table A1. Calculation of the surfaces of the cylindric fin piston.

Cylindric Fins			
D	2 × C	s_cyl	2 × s_cyl
27.5	22.5	7065	
27.5	17.5	5495	
27.5	12.5	3925	
27.5	7.5	2355	
27.5	2.5	785	
		19,625	39,250
	Surface of the cylinder fins		39,250
	Surface of the external cylinder		8639.379797
	Surface of the extremities		1187.3125
	Total_conv_surface		49,076.6923

References

1. Tian, H.; Zhang, H.; Yin, Z.; Liu, Y.; Zhang, X.; Xu, Y.; Chen, H. Advancements in compressed air engine technology and power system integration: A comprehensive review. *Energy Rev.* **2023**, *2*, 100050. [CrossRef]
2. Fazeli, A.; Khajepour, A.; Devaud, C. A novel compression strategy for air hybrid engines. *Appl. Energy* **2011**, *88*, 2955–2966. [CrossRef]
3. Rufer, A. *Semi-Rotary and Linear Actuators for Compressed Air Energy Storage and Energy Efficient Pneumatic Applications*; Bentham Science Publishers: Sharjah, United Arab Emirates, 2023.
4. Mahbod, H. Contribution to the Technique of Compressed Air Energy Storage—The Concept of Finned Piston. Ph.D. Thesis, Ecole Polytechnique Fédérale de Lausanne, Lausanne, Switzerland, 2015.
5. Chengel, Y.A.; Boles, M.A. *Thermodynamics: An Engineering Approach*, 6th ed.; McGrew-Hill Companies: New York, NY, USA, 2008; ISBN 978-0-07-352921-9.
6. Winterbone, D.E.; Turan, A. Chapter 2—The Second Law and Equilibrium. In *Advanced Thermodynamics for Engineers*, 2nd ed.; Butterworth-Heinemann: Oxford, UK, 2015; pp. 13–33, ISBN 9780444633736.
7. Brun, K.; Kurz, R. *Compression Machinery for Oil and Gas*; Elsevier Inc.: Amsterdam, The Netherlands, 2019; ISBN 978-0-12-814683-5. [CrossRef]
8. Yan, C.Y. *Introduction to Engineering Thermodynamics*; BC Campus: Victoria, BC, Canada, 2022.
9. Heidari, M.; Lemofouet, S.; Rufer, A. On The Strategies Towards Isothermal Gas Compression and Expansion. In Proceedings of the International Compressor Engineering Conference at Purdue, Lafayette, IN, USA, 14–17 July 2014.
10. Kim, T.; Lee, C.-Y.; Hwang, Y. *Reinhard Radermacher a Review on Nearly Isothermal Compression Technology*; Elsevier: Amsterdam, The Netherlands, 2022.
11. Rufer, A. Increasing the Energy Efficiency of Gas Boosters for Hydrogen Storage and for Refueling Stations. *Energies* **2023**, *16*, 1763. [CrossRef]
12. Vigen, A.; Jean-Paul, L.B.; Manuk, M. Design of Scotch Yoke Mechanisms with Improved Driving Dynamics. *Proc. Inst. Mech. Eng. Part K J. Multi-Body Dyn.* **2016**, *230*, 379–386.